

SUPPLEMENTAL MATERIAL

SUPPLEMENTAL METHODS

Microbubble Preparation

For murine experiments, lipid-shelled decafluorobutane microbubbles were prepared by sonication of a gas-saturated aqueous suspension of 2 mg/mL distearoylphosphatidylcholine and 1 mg/mL of distearoylphosphatidylethanolamine-PEG(2000). Microbubble concentration was measured by electrozone sensing (Multisizer III, Beckman Coulter) and electric surface potential (zeta potential) was determined by measurement of their electrophoretic mobility (ZetaPALS, Brookhaven Instruments, Holtsville, New York) in 1 mmol/l KCl at pH 7.4.

Cavitation Detection

Characterization of microbubble cavitation during therapeutic ultrasound exposure was assessed by passive cavitation detection (PCD). A spherically focused broadband (10 KHz to 20 MHz) hydrophone (Y-107, Sonic Concepts, Inc., WA) with a focal depth of 20 mm and a focal width of 0.4 mm was confocally positioned with the therapeutic ultrasound transducer at a 70° relative angle to receive signals from the proximal hindlimb during CEU. Received signals were digitized (25 MHz) and saved in a 4-channel oscilloscope (Waverunner, Teledyne LeCroy, Chestnut Ridge, NY) using sequence mode. Data analysis for 15 exposures for each condition was performed with the Matlab (MathWorks, Natick, MA). In order to differentiate inertial from stable cavitation, US exposure was performed at a mechanical index of 0.2 in addition to 1.3.

Ex Vivo Arterial Dilation

First order mesenteric arteries (n=7) were dissected free and removed from the omentum of Sprague-Dawley rats, cannulated at each end, and placed in an tissue bath. Arterial diameter was measured with high frequency (38 MHz) ultrasound (VisualSonics Inc.) performed with transducer alignment co-axial to the vessel. Baseline arterial diameter (average of three separate locations within the vessel) was measured after a two minute continuous perfusion at 0.6 ml/min (Newtonian shear rate of $\approx 700 \text{ s}^{-1}$) with isothermic Krebs-Henseleit buffer containing MBs ($5 \times 10^7 \text{ mL}^{-1}$) at a concentration to replicate *in vivo* immediate post-injection concentrations assuming a 2 mL blood volume of distribution. Diameter measurements were then repeated upon completion of ultrasound cavitation for 2 min produced by long-axis exposure of the artery to ultrasound (Sonos 7500, Philips Ultrasound) at 5 second intervals using harmonic power-Doppler at 1.3 MHz, a Doppler pulse repetition frequency of 9.3 kHz, and an MI of 1.3. Once the vessel was allowed to return to baseline, studies were repeated using Krebs-Henseleit buffer containing RBCs (6:4 v:v) and MBs.

Assessment of Cellular Poration.

Microvascular endothelial cells (SVEC4-10) were grown to confluence on 35 mm culture dishes. MBs (1×10^8) were added to the culture medium, dishes were inverted, and cells were exposed to therapeutic US for 1 min using conditions described above at a mechanical index of 1.1 and a frame rate of 1 Hz. To assess for microporation, propidium iodide (PI) at a final concentration of 20 $\mu\text{g/mL}$ was added to the medium at the time of US exposure. To assess for both resolution of microporation and loss of viability (defined by persistent cell membrane permeability), experiments were also performed with a 10 or 20 min delay in adding propidium iodide after US. Dioctadecyl-tetramethylindocarbocyanine perchlorate (DiI) was added to the

Belcik T, et al.

cells to define cell borders and fluorescent microscopy was performed to determine the number of cells per optical field (0.4 mm^2) with positive nuclear PI staining. For evaluation of RBC poration, citrated whole blood was obtained from normal volunteers. Blood (0.5 mL) was combined with 1.5 mL of 3 mg/mL fluorescein isothiocyanate-labeled (FITC-) dextran (MW 40,000) (Sigma-Aldrich, St. Louis, MO) in 0.9% NaCl and with 5×10^8 microbubbles. Cells were exposed to US as described above or similar amount of time without US for control conditions. A separate set of cells were studied with a 20 min delay in adding FITC-dextran to the cells after US. Cells were washed 4-times and evaluated by flow cytometry (FACSCanto II, BD Biosciences) gated to the erythrocyte population at 488 nm excitation and displayed as histograms of fluorescent intensity.

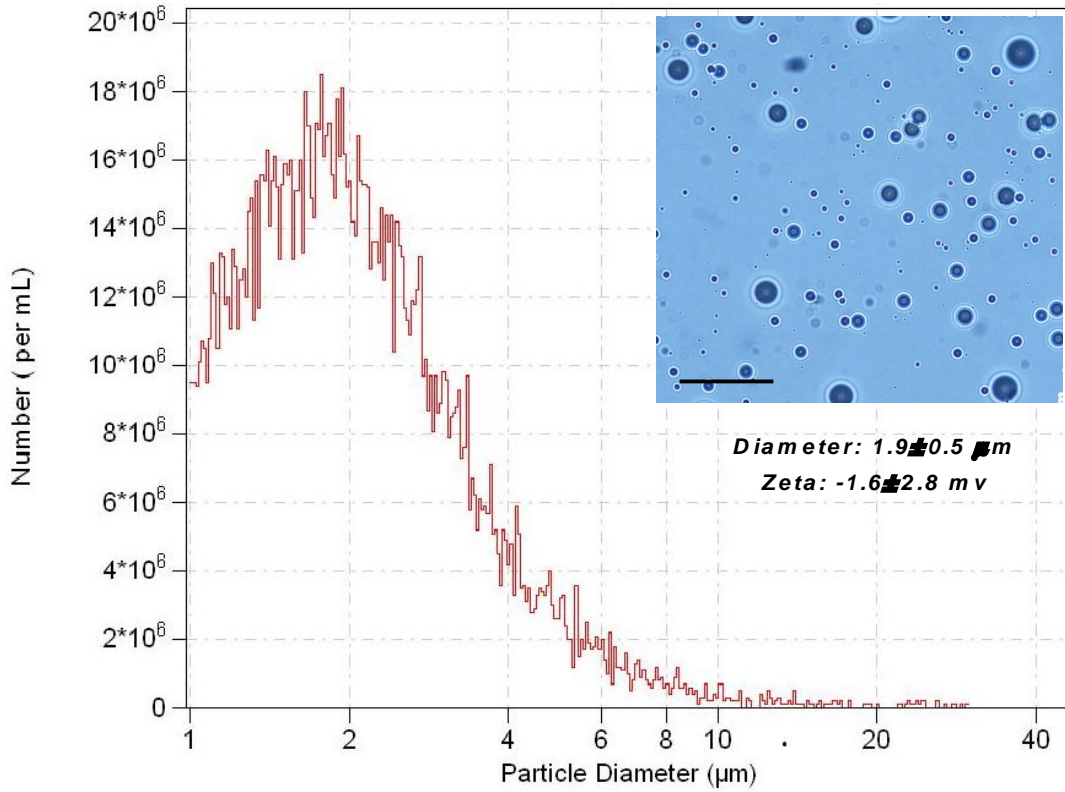
RBC Deformability.

Human RBCs were obtained from normal volunteers, washed, and 1 mL was diluted 1:2 with phosphate buffered saline. MBs were added to a final concentration of $5 \times 10^8 \text{ mL}^{-1}$ and exposed to exposed to therapeutic US for 1 min using conditions described above at a mechanical index of 1.1 and a frame rate of 1 Hz. Twenty-five microliters of the RBC suspension was mixed with 5 mL of polyvinyl propylene (50 mg/mL). Erythrocyte deformability at variable shear was evaluated using laser-assisted optical rotational cell analysis (LORRCA, Mechatronics) at shear stresses from 1.7 to 16.9 Pa and expressed as an elongation index (EI) which was calculated from the ratio of the axial and transverse erythrocyte diameters relative to the direction of shear.

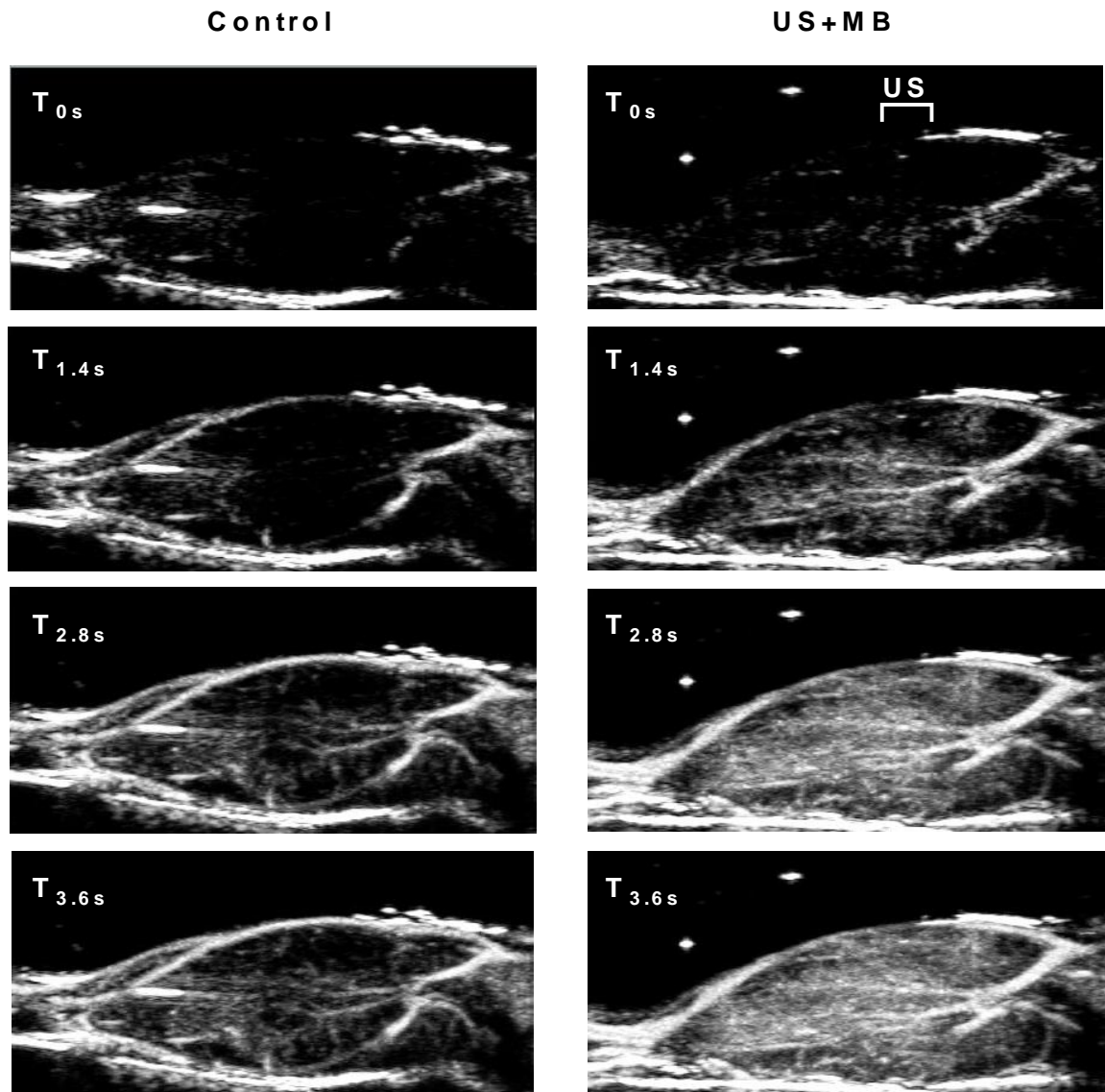
Statistical Methods

Statistical analysis was made with Prism (v. 6.02, GraphPad Inc., La Jolla, CA). Data are expressed as \pm SD unless stated otherwise. D'Agostino and Pearson omnibus test were used to assess data normality. Significance for variance among multiple (>2) groups was analyzed with one-way ANOVA and, when significant ($p < 0.05$), post-hoc analysis was performed with unpaired Student's *t*-test with Bonferroni's correction when applicable. Paired comparisons of normally distributed data (pre- vs. post-exposure; treated vs. untreated leg in normal and ischemic limbs) were made with unpaired Student's *t*-test. Repeated measures ANOVA was used to assess the temporal blood flow response in ischemic limbs. Non-normally distributed data were analyzed with a Mann-Whitney U test except for comparisons of eNOS phosphorylation between treated and contralateral leg which were analyzed by a Wilcoxon signed-rank test. Curve fitting for CEU data was performed using weighted non-linear regression models.

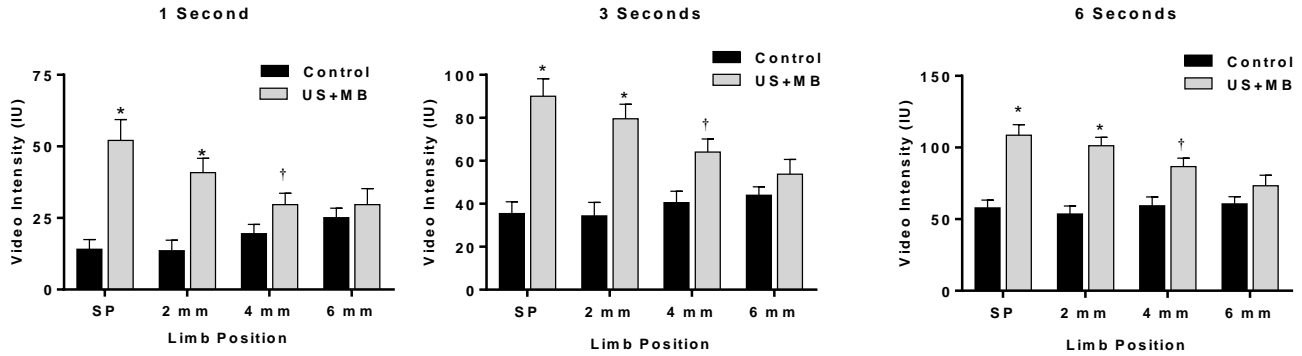
SUPPLEMENTAL FIGURES AND LEGENDS



Supplemental Figure 1. Microbubble Diameter Measurement. Example of electrozone sensing of microbubble diameter distribution and light microscopy imaging (inset) of microbubbles (scale bar = 20 μm). Average mean diameter and zeta potential of microbubbles used for this study is provided.

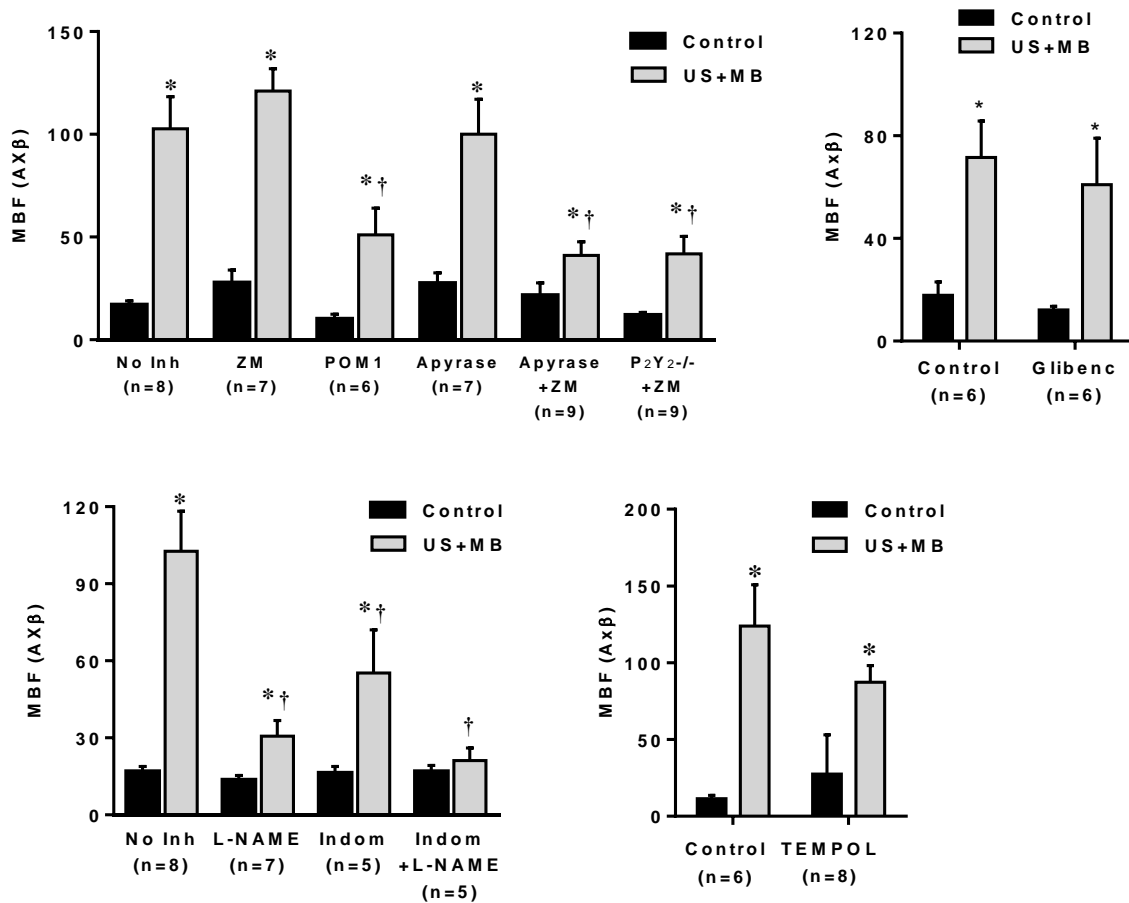


Spatial Assessment of Flow Augmentation. CEU perfusion imaging in the long-axis of the proximal hindlimb with MIP projection imaging in the control limb and the limb exposed to cavitation energy (US+MB). The proximal portion of the limb is to the left and the bracket illustrates the location of the transaxial therapeutic ultrasound plane. Images show temporal sequences of contrast replenishment after a destructive pulse sequence illustrating hyperemia encompassing the entire proximal hindlimb of the US+MB subject.



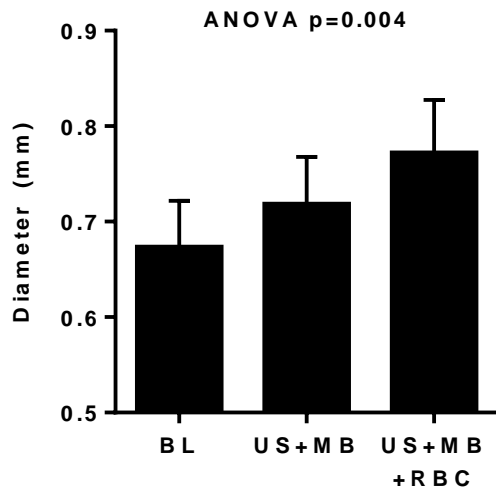
Supplemental Figure 3. MIP Data With Varying Temporal Delays. MIP Mean (\pm SEM) intensity data obtained 1 s, 3 s, and 6 s into the maximum intensity projection imaging acquisition from the control and US-exposed (*US+MB*) non-ischemic limbs (n=14). Imaging was performed with a 90-degree rotation from therapeutic US plane 10 min after therapeutic US and illustrates distribution of perfusion within the 2 mm-wide therapeutic US sector plane (*SP*) and distal adjacent sectors at 2, 4, and 6 mm increments. * $p < 0.01$ vs control limb; † $p \leq 0.05$ versus control.

Supplemental Figure 4

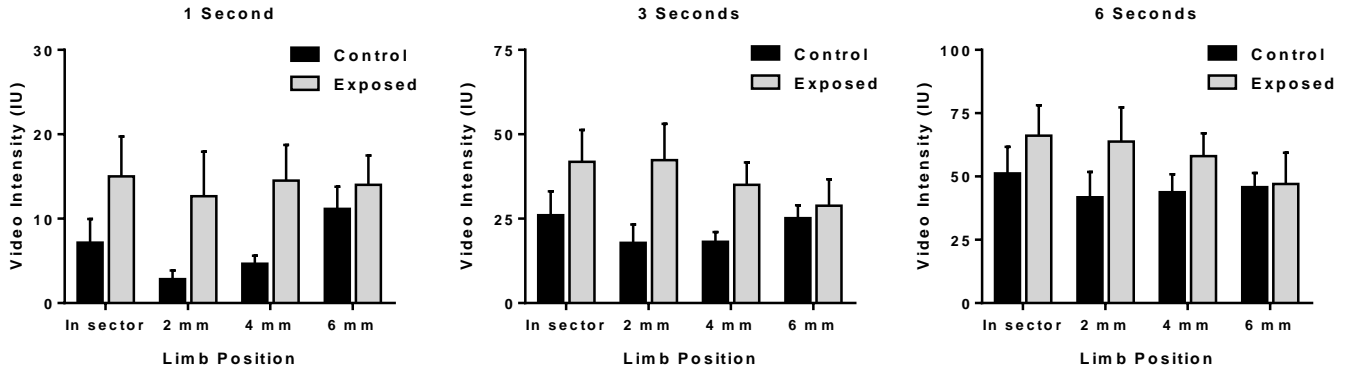


Supplemental Figure 4. Mechanism of Muscle Flow Augmentation During US cavitation. (a) Mean (±SEM) microvascular blood flow in contralateral control and US-exposed (*US+MB*) limbs in wild-type control mice without inhibitors (*No Inh*); in wild-type mice pre-treated with inhibitors to vasoactive pathways (see text); and in *P2Y2*^{-/-} mice treated with the adenosine *A*_{2a} receptor antagonist ZM241385 (*ZM*). **p*<0.05 vs control; †*p*<0.05 versus no inhibitor. (b) Mean (±SEM) microvascular blood flow in contralateral control and US-exposed limbs in wild-type mice with and without pre-treatment with glibenclamide. **p*<0.05 versus control. (c) Mean (±SEM) microvascular blood flow in control and US-exposed limbs in wild-type mice in mice pre-treated with L-NAME, indomethacin, or L-NAME and indomethacin. **p*<0.0001 vs control; †*p*<0.05 vs control and *p*<0.001 vs no inhibitor. (e) Mean (±SEM) microvascular blood flow in control and US-exposed limbs in wild-type mice without inhibitors or pre-treated with TEMPOL. **p*<0.01 vs control.

Supplemental Figure 5.



Supplemental Figure 5. Arterial Dilation During Cavitation. Mean (\pm SEM) diameter of rat mesenteric arteries assessed during *ex vivo* perfusion studies (n=7). Baseline (BL) conditions were after 2 min of perfusion with Krebs-Henseilet buffer. Post-cavitation data were obtained in the absence (US+MB) and presence of RBCs.



Supplemental Figure 6. MIP Data in Ischemic Limbs. Mean (\pm SEM) intensity data obtained 1 s, 3 s, and 6 s into the maximum intensity projection imaging acquisition from the control non-ischemic and non-exposed, and US-exposed (*US+MB*) ischemic limbs (n=6). Imaging was performed with a 90-degree rotation from therapeutic US plane 10 min after therapeutic US and illustrates distribution of perfusion within the 2 mm-wide therapeutic US sector plane (*SP*) and distal adjacent sectors at 2, 4, and 6 mm increments.